

Performance Analysis of Grooved Hydrodynamic Journal Bearing with Multi-Depth Textured Surface

K.M. Faez^a, S. Hamdavi^b, T.V.V.L.N. Rao^c, H.H. Ya^d and Norani M. Mohamed^e

Dept. of Mech. Engg., Universiti Teknologi Petronas, Seri Iskandar, Perak, Malaysia

^aEmail: kumuhammadfaez@gmail.com

^bEmail: shahab.hamdavi@yahoo.com

^cEmail: tvlnrao@gmail.com

^dCorresponding Author, Email: hamdan.ya@utp.edu.my

^eEmail: noranimuti_mohamed@utp.edu.my

ABSTRACT:

In recent research, theoretical studies and investigations for the textured surface of a hydrodynamic journal bearing has been widely used. This is due to the journal bearing's performance in terms of load capacity which affects the system performance, efficiency and reliability. It has been proven that a textured surface and grooved surface have managed to improve the performance of journal bearings to some extent. In this work, the performance of a grooved hydrodynamic journal bearing has been analysed with a multi-depth textured surface. The study has been conducted using the modified Reynolds equation to numerically solve the load capacity and pressure distribution, respectively. From the results obtained, it was found that the surface complexity features on the journal bearing lowered the load capacity performance when compared to the plain bearing. The pressure, meanwhile, was distributed throughout the textured sections on the bearing surface, even though it was lower as compared to the plain bearing.

KEYWORDS:

Surface texture; Load capacity; Hydrodynamic journal bearings

CITATION:

K.M. Faez, S. Hamdavi, T.V.V.L.N. Rao, H.H. Ya and Norani M. Mohamed. 2018. Performance analysis of grooved hydrodynamic journal bearing with multi-depth textured surface, *Int. J. Vehicle Structures & Systems*, 10(2), 142-145. doi:10.4273/ijvss.10.2.13.

1. Introduction

A bearing is a type of mechanical device that allows relative movement between two mechanical parts. In hydrodynamic contacts of journal bearings, the effect of the surface texturing and a grooved surface being applied has increased the attention to it as it will affect the performance of a journal bearing like on the load capacity, pressure distribution, and friction coefficient. Tonder [1] studied the effect of the roughening on both the inlet and outlet areas of the journal bearing, which proved the increase of load capacity. Pratibha and Chandresh Kumar [2], in another work, performed a study of the effect of a textured surface on the hydrodynamic performance of a journal bearing. The research was undertaken in regards to the journal speed and the texture context with various load conditions, where the pressure and load increased significantly. Similar research work was also carried out by Kango et al [3]. They investigated the micro cavities present in finite journal bearings as different cavity locations significantly enhance bearing performance. Tala-Ighil et al [4] used the FDM approach which proved that the proper configuration of the surface texture does help to improve lubrication contact. However, applying a fully textured surface could lead to a decrease in the performance as mentioned by Buscaglia et al [5]. In their

research findings, the hydrodynamic performance of the bearing was decreased as all of the bearing's surface was applied with texture. Tauviquirrahman et al [6] modified the governing Reynolds equation to investigate the partial texturing and slip effect on a slider bearing; the results led to interest in applying partial texturing in hydrodynamic lubrication.

Etsion et al [7] performed an experimental analysis and concluded that a partially textured surface can be made by using laser surface texturing (LST) that improves the thrust bearing's performance. To increase the effectiveness of the surface texture in hydrodynamic contacts, Yu et al [8] studied various types of partial textures that were the most suitable to improve the load capacity of a journal bearing. Hamdavi et al [9], meanwhile analysed the surface texturing effect on the load capacity and film pressure of hydrodynamic journal bearing performance. Rao et al [10] performed another study using the configuration of a partial texture and partial slip with grooves on the hydrodynamic performance of slider and journal bearings using another model of study. Another similar study has also been carried out by Faez et al [11] in which they investigated the effect of surface texturing with slip and no slip surfaces on grooved hydrodynamic journal bearing performance. In their research, it was proven that surface texturing with grooved and also slip/no-slip conditions did improve the load capacity of the bearing.

In this paper, an analysis has been conducted which used a grooved hydrodynamic journal bearing with a multi-depth textured surface. It has been aimed to determine the change of the performance of the bearing's load capacity towards different eccentricity ratios. The objective of this research was to analyse the effect of the multi-depth textured surface with different parameters on the load capacity and pressure distribution of the grooved hydrodynamic journal bearing by using a modified Reynolds equation. The multi-depth surface texture consisted of two steps of the recessed region that will be discussed later.

2. Methodology

In this work, the load capacity of a grooved hydrodynamic journal bearing of a multi-depth surface texture, as shown in Fig. 1, is calculated. In this approach, the Reynolds equation and boundary conditions were applied and the numerical analysis was carried out as performed by Faez et al [11]. The boundary condition of the two-step textured surface was defined where the recess area was divided into two sections which were the 1st and 2nd steps. The angular length of the 1st step recess area is given by,

$$\theta_{1,2} - \theta_{1,1} = \theta_{r1} \text{ or } \theta_{n,2} - \theta_{n,1} = \theta_{r1} \quad (1)$$

Meanwhile, the 2nd step of the recess area was as,

$$\theta_{1,3} - \theta_{1,2} = \theta_{r2} \text{ or } \theta_{n,3} - \theta_{n,2} = \theta_{r2} \quad (2)$$

On the other hand, the angular length for the land area (plain surface) was defined as,

$$\theta_{1,4} - \theta_{1,3} = \theta_n \text{ or } \theta_{n,4} - \theta_{n,3} = \theta_n \quad (3)$$

The thickness of the film at the 1st and 2nd step recess areas were H' and H'' respectively are,

$$H = (1 + \varepsilon \cos \theta), H' = H + H_g \text{ and } H'' = H + \frac{1}{2} H_g \quad (4)$$

The modified Reynolds equation for the partially textured surface is,

$$\frac{d}{d\theta} \left[\frac{H^4}{12H} \frac{dp}{d\theta} \right] = \frac{1}{2} \frac{d}{d\theta} H \quad (5)$$

The boundary conditions for the pressure at the bearing surface are defined as,

$$P|_{\theta=0} = 0, P|_{\theta=\theta_{1,2}} = P_{1,2}, P|_{\theta=\theta_{1,3}} = P_{1,3}, P|_{\theta=\theta_{1,4}} = P_{1,4} \quad (6)$$

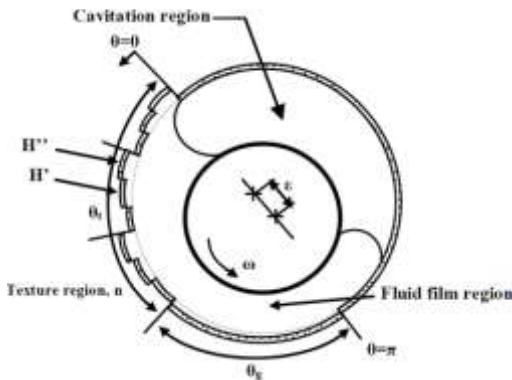


Fig. 1: Two-step surface texture configuration on a grooved hydrodynamic journal bearing

Integrating Eqn. (4) yielded the dimensionless pressure profiles of the textured region, θ_t ,

$$1^{\text{st}} \text{ step grooved region: } \frac{dP}{d\theta} = \frac{6}{H'^2} - \frac{12Q}{H'^3} \quad (7)$$

$$2^{\text{nd}} \text{ step grooved region: } \frac{dP}{d\theta} = \frac{6}{H''^2} - \frac{12Q}{H''^3} \quad (8)$$

$$\text{Plain surface region: } \frac{dP}{d\theta} = \frac{6}{H^2} - \frac{12Q}{H^3} \quad (9)$$

Integrating Eqns. (7-9) with the substitution of the boundary conditions in Eqn. (6) gave the dimensionless pressure profiles of the textured region as,

$$P(0 \leq \theta \leq \theta_{1,2}) = P|_{\theta=0} + 6 \int_0^{\theta_{1,2}} \frac{1}{H'^2} d\theta - 12 \int_0^{\theta_{1,2}} \frac{1}{H'^3} d\theta \quad (10)$$

$$P(\theta_{1,2} \leq \theta \leq \theta_{1,3}) = P|_{\theta=1,2} + 6 \int_{\theta_{1,2}}^{\theta_{1,3}} \frac{1}{H''^2} d\theta - 12 \int_{\theta_{1,2}}^{\theta_{1,3}} \frac{1}{H''^3} d\theta \quad (11)$$

$$P(\theta_{1,3} \leq \theta \leq \theta_{1,4}) = P|_{\theta=1,3} + 6 \int_{\theta_{1,3}}^{\theta_{1,4}} \frac{1}{H^2} d\theta - 12 \int_{\theta_{1,3}}^{\theta_{1,4}} \frac{1}{H^3} d\theta \quad (12)$$

The dimensionless pressure was substituted and simplified using the pressure from the previous Eqns. From there, the flow volume, Q is determined as,

$$Q = \frac{\sum_4 \left(\int_{\theta_{1,1}}^{\theta_{1,2}} \frac{1}{H'^2} d\theta + \int_{\theta_{1,2}}^{\theta_{1,3}} \frac{1}{H''^2} d\theta + \int_{\theta_{1,3}}^{\theta_{1,4}} \frac{1}{H^2} d\theta \right) + \int_{\theta_1}^{\theta_2} \frac{1}{H'^2} d\theta}{\sum_4 \left(\int_{\theta_{1,1}}^{\theta_{1,2}} \frac{2}{H'^3} d\theta + \int_{\theta_{1,2}}^{\theta_{1,3}} \frac{2}{H''^3} d\theta + \int_{\theta_{1,3}}^{\theta_{1,4}} \frac{2}{H^3} d\theta \right) + \int_{\theta_1}^{\theta_2} \frac{2}{H'^3} d\theta} \quad (13)$$

Next, the dimensionless pressure across the centre line is integrated and yield the radial and tangential load capacity as expressed below,

$$W_\varepsilon = \left[\begin{array}{l} - \left(\int_{\theta_{1,1}}^{\theta_{1,2}} P_1 \cos(\theta) d\theta + \int_{\theta_{1,2}}^{\theta_{1,3}} P_2 \cos(\theta) d\theta + \right. \\ \left. \int_{\theta_{1,3}}^{\theta_{1,4}} P_3 \cos(\theta) d\theta + \dots + \int_{\theta_1}^{\theta_2} P_7 \cos(\theta) d\theta \right) \end{array} \right] \quad (14)$$

$$W_\phi = \left[\begin{array}{l} - \left(\int_{\theta_{1,1}}^{\theta_{1,2}} P_1 \sin(\theta) d\theta + \int_{\theta_{1,2}}^{\theta_{1,3}} P_2 \sin(\theta) d\theta + \right. \\ \left. \int_{\theta_{1,3}}^{\theta_{1,4}} P_3 \sin(\theta) d\theta + \dots + \int_{\theta_1}^{\theta_2} P_7 \sin(\theta) d\theta \right) \end{array} \right] \quad (15)$$

From the radial and tangential load capacities obtained, the dimensionless load capacity is calculated as,

$$W = \sqrt{W_\varepsilon^2 + W_\phi^2} \quad (16)$$

3. Result and discussion

To evaluate the performance of the load carrying capacity and dimensionless pressure distribution in the two-step surface texture in a grooved hydrodynamic journal bearing, some parameters were defined and considered accordingly. These parameters were - the eccentricity ratio (ε) ranging from 0.1 to 0.8, with a 0.1 increment; dimensionless groove depth (H_g) with values of 0.2, 0.5, and 0.8; surface texture length, (θ_t) region which had the values of 40°, 80°, and 120°; groove to land ratios (γ), which was noted as 0.2, 0.4, 0.6, and 0.8 and: (n) the number of grooved regions applied, which were noted as 2, 4, 6, and 8. Fig. 2 shows that the lower groove to land ratio magnitude (γ) had a slightly better load capacity compared to the higher groove to land ratio. However, comparing this to the plain bearing in terms of overall performance, it is still lower due to the complex features on the bearing surface. A similar comparison can also be seen with the pressure

distribution in Fig. 6 as the pressure distribution of the multi-depth textured surface was lower than the plain bearing distribution; in addition, the texture feature produced some pressure changes along the circumferential angle. Fig. 3 shows a graph reading over the groove depth. In general, the smaller groove depth produced a better load capacity compared to the deeper depth. Despite the increase, it was still lower than the plain bearing. The lower groove depth has minimised the complexity of the textured surface thus leading to a better load capacity. Similar explanation can also be inferred from Fig. 7 as the lower groove depth had a better pressure distribution along the circumferential angle, even though it was lower when compared to the plain bearing performance.

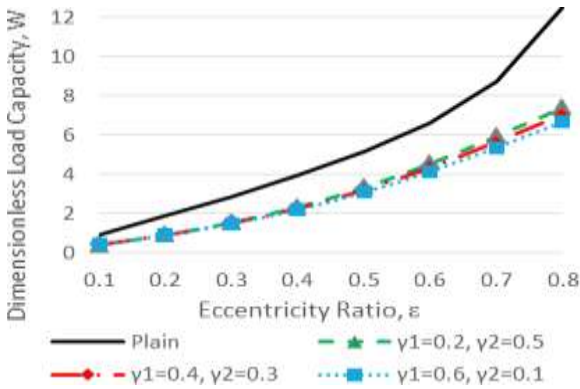


Fig. 2: Load capacity of γ at $\theta_g = 170^\circ$, $\theta_t = 120^\circ$, $H_g = 1$, $n = 4$

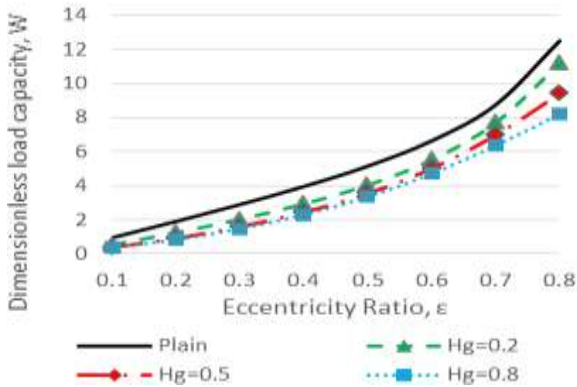


Fig. 3: Load capacity of H_g at $\theta_g = 170^\circ$, $\theta_t = 120^\circ$, $n = 4$, $\gamma = 0.3$

For the number of textured regions, the (n) parameter, as shown in Fig. 4 and Fig. 8, it can be seen that the change of the textured regions produced a very small difference in the load capacity. The only difference that can be seen is that, at the pressure distribution in Fig. 8, as the number of the pressure changed it was different due to the different numbers of textured regions present on the bearing's surface. Overall, both the load capacity and the pressure distribution were lower compared to the plain bearing performance. For the last parameter, which involved the texture length (θ_t) as shown in Fig. 5 and Fig. 9, the load capacity had a slight difference at the lower eccentricity and high eccentricity regions in which a shorter texture length had a better load capacity at the low eccentricity. However, the load capacity was better with the longer texture length. Despite the load capacity being lower than the plain bearing, the pressure distribution seemed to have a minor discovery, which was that, at the texture length greater

than 120° , the pressure distribution was much higher at the grooved region (θ_g). Meanwhile, the textured surface region (θ_t) produced almost a similar pressure distribution pattern when compared to the other parameters.

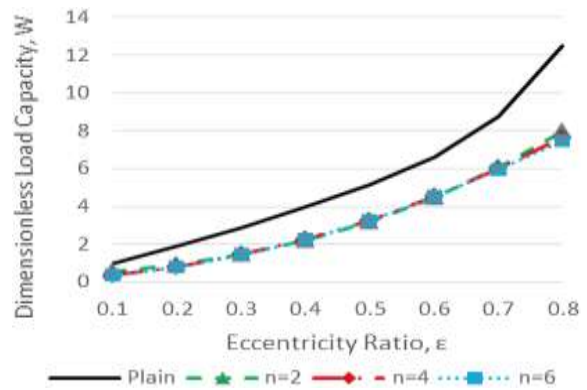


Fig. 4: Load capacity of n at $\theta_g = 170^\circ$, $\theta_t = 120^\circ$, $H_g = 1$, $\gamma = 0.3$

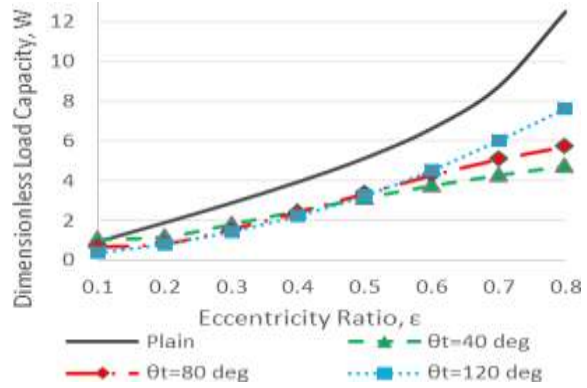


Fig. 5: Load capacity of θ_t at $\theta_g = 170^\circ$, $H_g = 1$, $\gamma = 0.3$, $n = 4$

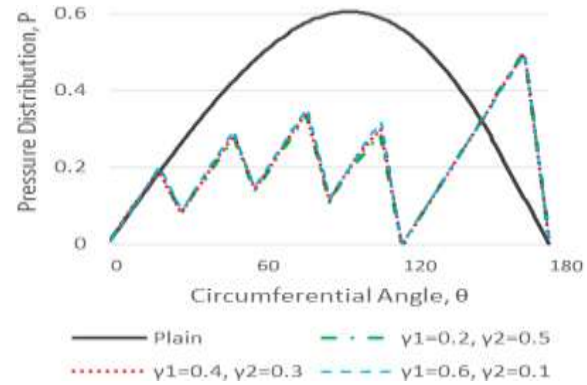


Fig. 6: Pressure distribution of γ at $\theta_g = 170^\circ$, $\theta_t = 120^\circ$, $H_g = 1$, $n = 4$

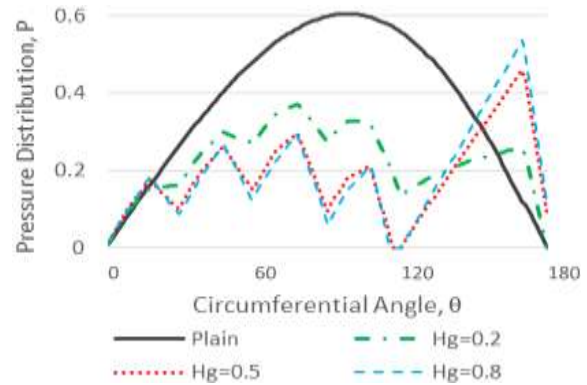


Fig. 7: Pressure distribution of H_g at $\theta_g = 170^\circ$, $\theta_t = 120^\circ$, $n = 4$, $\gamma = 0.3$

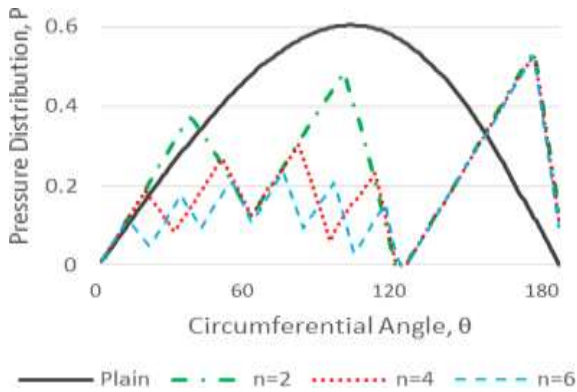


Fig. 8: Pressure distribution of n at $\theta_g = 170^\circ$, $\theta_t = 120^\circ$, $H_g = 1$, $\gamma = 0.3$

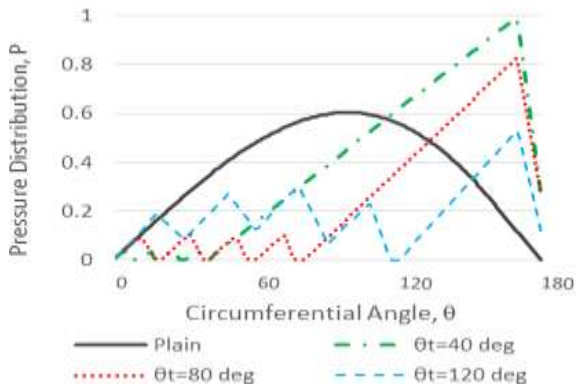


Fig. 9: Pressure distribution of θ_t at $\theta_g = 170^\circ$, $H_g = 1$, $\gamma = 0.3$, $n = 4$

4. Conclusion

This study has investigated the effect of a multi-depth textured surface in grooved hydrodynamic journal bearings in regards to the load carrying capacity and pressure distribution. Based on the analysis undertaken, the following conclusions are drawn,

- Overall, the load capacity and pressure distribution for the multi-depth textured bearing is lower compared to the plain bearing due to its surface complexity presence on the bearing.
- Lowering the groove depth significantly improves load capacity as it reduces the surface complexity of the textured region on the bearing.
- The presence of multi-depth surface textures distributes the pressure along the circumferential angle more evenly as compared to the plain bearing in which the pressure is stressed at the middle region (90°).

ACKNOWLEDGEMENTS:

The authors would like to thank the Ministry of Higher Education Malaysia for their kind support of this research. The research project is under the Fundamental Research Grant Scheme; FRGS-0153AB-K49.

REFERENCES:

- [1] K. Tonder. 2001. Inlet roughness tribodevices: Dynamic coefficients and leakage, *Tribology Int.*, 34(12), 847-852. [https://doi.org/10.1016/S0301-679X\(01\)00084-6](https://doi.org/10.1016/S0301-679X(01)00084-6).
- [2] S. Pratibha and P.R. Chandreshkumar. 2014. Effect of bearing surface texture on journal bearing pressure distribution, *Int. J. Science and Research*, 3(6), 2223-2226.
- [3] S. Kango, D. Singh and R. Sharma. 2012. Numerical investigation on the influence of surface texture on the performance of hydrodynamic journal bearing, *Meccanica*, 47(2), 469-482. <https://doi.org/10.1007/s11012-011-9460-y>.
- [4] N. Tala-Ighil, M. Fillon and P. Maspeyrot. Effect of textured area on the performances of a hydrodynamic journal bearing, *Tribology Int.*, 44(3), 211-219. <https://doi.org/10.1016/j.triboint.2010.10.003>.
- [5] G.C. Buscaglia, I. Ciuperca and M. Jai. 2007. On the optimization of surface textures for lubricated contacts, *J. Mathematical Analysis and Applications*, 335(2), 1309-1327. <https://doi.org/10.1016/j.jmaa.2007.02.051>.
- [6] M. Tauviquirrahman, R. Ismail, J. Jamari and D.J. Schipper. 2013. A study of surface texturing and boundary slip on improving the load support of lubricated parallel sliding contacts, *Acta Mechanica*, 224(2), 365-381. <https://doi.org/10.1007/s00707-012-0752-7>.
- [7] I. Etsion, G. Halperin, V. Brizmer and Y. Kligerman. 2004. Experimental investigation of laser surface textured parallel thrust bearings, *Tribology Letters*, 17(2), 295-300. <https://doi.org/10.1023/B:TRIL.0000032467.88800.59>.
- [8] R. Yu, P. Li and W. Chen. 2016. Study of grease lubricated journal bearing with partial surface texture, *Industrial Lubrication and Tribology*, 68(2), 149-157. <https://doi.org/10.1108/ILT-03-2015-0028>.
- [9] S. Hamdavi, H. Ya and T. Rao. 2016. Effect of surface texturing on hydrodynamic performance of journal bearings, *ARPJ J. Engg. and Appl. Scis.*, 11(1), 172-176.
- [10] T. Rao, A. Rani, T. Nagarajan and F. Hashim. 2012. Analysis of slider and journal bearing using partially textured slip surface, *Tribology Int.*, 56, 121-128. <https://doi.org/10.1016/j.triboint.2012.06.010>.
- [11] K. Faez, S. Hamdavi, H. Ya and T. Rao. 2016. An analytical investigation of the grooved journal bearing's performance with slip/no-slip texture bearing, *ARPJ J. Engg. and Appl. Scis.*, 11(22), 12990-12993.